

1 **Supplementary Material**

2 **Supplement S1: Sensitivity Studies**

3 Figure S1 illustrates the concentration profiles for ozone and oleic acid when assuming constant
4 diffusivity in the semi-solid 12-component aerosol matrix. The differences to the diffusivity-
5 evolution model variant (see Fig. 5) are subtle, but accumulate to considerable differences in the
6 total loss in particular at long reaction times.

7 The sensitivity of our best-fit scenario (see solid lines in Fig. 1) is tested towards a wide range of
8 input parameters. Fig. S2 illustrates the impact of a 10-fold change of the surface rate
9 coefficients and Fig. S3 shows the impact of a 10-fold change of the bulk reactivity. The surface
10 reactivity has only a small impact on the total number of molecules lost (partly caused by the
11 surface to volume ratio of a 275nm-radius particle). The faster the surface reaction the slower
12 is the loss of the reactive component: this suggests that the loss is not limited by surface
13 reactivity, but by transport to the aerosol bulk. Surface rate coefficients are constrained by
14 experimental data (Pfrang et al., 2011) for ozonolysis of a monolayer of the oleic acid methyl
15 ester, methyl oleate. This new experimental evidence demonstrates considerably higher
16 reactivity at the surface than assumed previously (e.g. Pfrang et al., 2010) based on earlier
17 experimental work. The bulk rate coefficients affect the loss of reactive species significantly.
18 Please note that the bulk rate coefficients used in the best-fit scenario are constrained by
19 experimental data from Huff Hartz et al. (2007).

20 We also tested the sensitivity of our modelling approach on the method used to describe the
21 evolution of diffusivity. Throughout the paper we follow the obstruction theory approach
22 (Stroeve, 1975). In Fig. S4 we present an alternative approach using a linear combination
23 expression for the time-dependent diffusion coefficients assuming a product diffusivity of $\frac{1}{4}$ of
24 the initial value (based on a M^2 dependence for dimer formation; compare Bird et al., 2007).
25 There is a measurable, but not substantial difference between the two approaches (compare
26 Figs. 4 and S4) and we thus used the obstruction theory approach which has been applied in the
27 past (Stroeve, 1975).

28 The robustness of the model to the thickness of the layers representing the 275nm-radius
29 aerosol particle is illustrated in Fig. S5. The results converge from ca. 100 bulk layers with the
30 chosen 250 layers being both physically meaningful and computationally affordable.

31 **References**

32 Bird, R. B., Stewart, W. E., & Lightfoot, E. N.: *Transport Phenomena (2nd Ed.)* (John Wiley & Sons,
33 Inc., New York), 2007.

- 34 Huff Hartz, K. E. H., Weitkamp, E. A., Sage, A. M., Donahue, N. M. and Robinson, A. L.: Laboratory
35 measurements of the oxidation kinetics of organic aerosol mixtures using a relative rate
36 constants approach, *J. Geophys. Res.-Atmos.*, 112, D04204, 10.1029/2006jd007526, 2007.
- 37 Pfrang, C., Shiraiwa, M. and Pöschl, U.: Coupling aerosol surface and bulk chemistry with a
38 kinetic double layer model (K2-SUB): an exemplary study of the oxidation of oleic acid by
39 ozone, *Atmos. Chem. Phys.*, 10, 4357-4557, 2010.
- 40 Pfrang, C. et al.: Kinetics and mechanism of the reaction of ozone with a monolayer of *d*-methyl
41 oleate at the air-water interface studied by fast neutron reflectometry, in preparation, 2011.
- 42 Stroeve, P.: On the Diffusion of Gases in Protein Solutions, *Ind. Eng. Chem. Fund*, 14, 140-141,
43 1975.
- 44

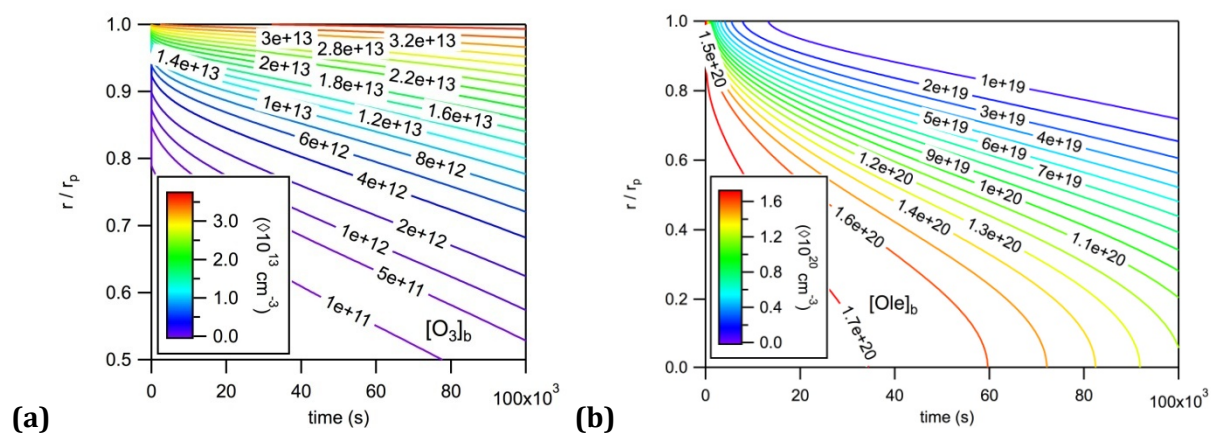


Figure S1 Concentration profiles of ozone ((a)) and oleic acid ((b)) when assuming constant-diffusivity of the semi-solid aerosol matrix. Equivalent profiles for the diffusivity-evolution model variant are displayed in Fig. 5 (a) and (b).

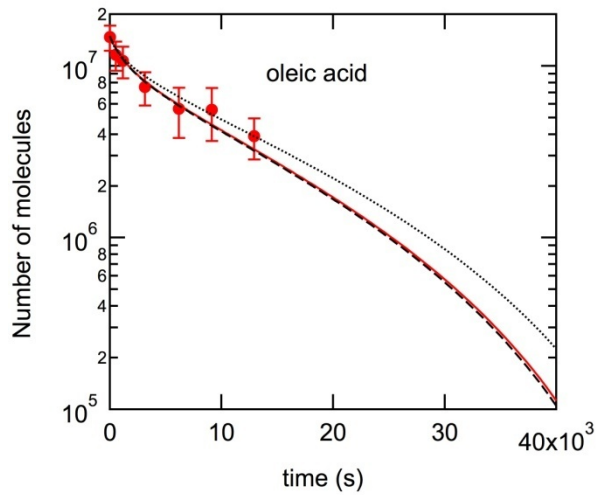


Figure S2 Decays of numbers of molecules of oleic acid in a 12-component aerosol matrix as a function of time. Symbols correspond to experimental data (Huff Hartz et al., 2007). Surface rate coefficients are set to be 10-fold higher (dotted line) and 10-fold lower (dashed line) than in our best-fit scenario (red solid line).

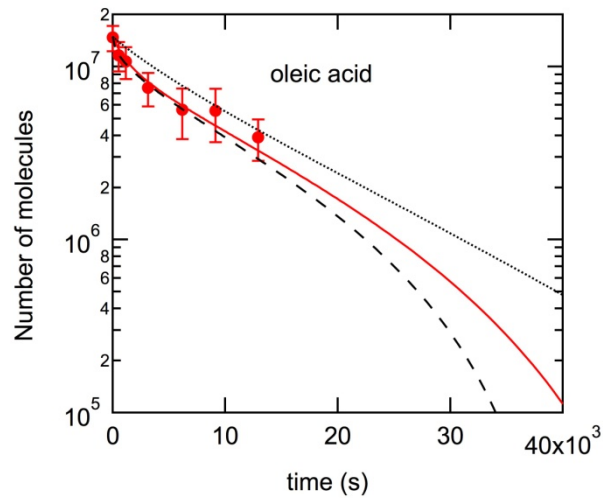


Figure S3 Decays of numbers of molecules of oleic acid in a 12-component semi-solid aerosol matrix as a function of time. Symbols correspond to experimental data (Huff Hartz et al., 2007). Bulk rate coefficients are set to be 10-fold higher (dashed line) and 10-fold lower (dotted line) than in our best-fit scenario (red solid line).

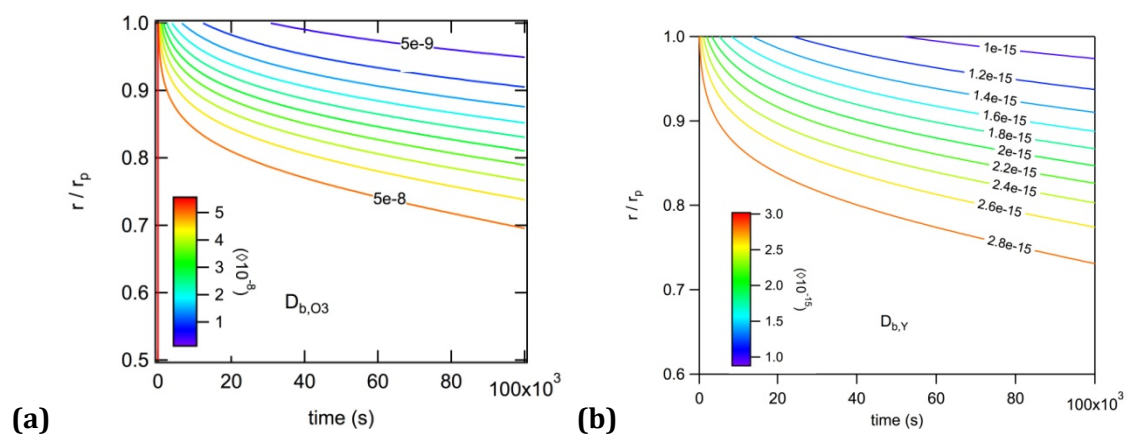


Figure S4 Bulk diffusion coefficients of (a) ozone and (b) oleic acid as a function of time and depth in the 275nm-radius particle. The diffusivity evolution is represented here by a linear combination assuming a final diffusion coefficient at $\frac{1}{4}$ of the initial coefficient. Fig. 4 shows the equivalent plots with the diffusivity expressed by obstruction theory (Stroevé, 1975).

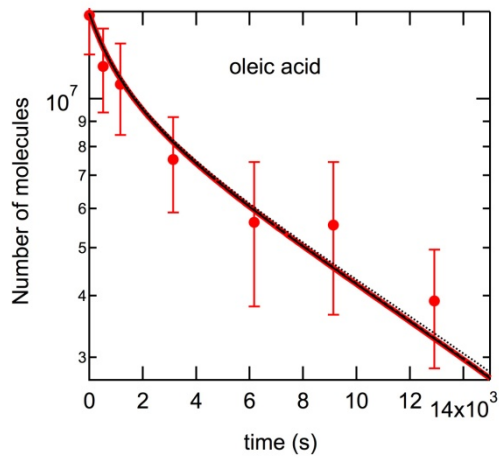


Figure S5 Decays of numbers of molecules of oleic acid in a 12-component aerosol matrix as a function of time. Symbols correspond to experimental data (Huff Hartz et al., 2007). Numbers of layers representing the aerosol particle in the model are varied ($n = 50$ -275; black lines; the dotted line slightly above the other lines is for $n = 50$). The bold red line corresponds to the model representation used for all other runs (see also solid line in Fig. 1 (a)) with $n = 250$.